



Published in final edited form as:

Neuroimage Rep. 2025 June ; 5(2): . doi:10.1016/j.ynrp.2025.100265.

Cerebral arterial lumens are enlarged in children and young adults with sickle cell disease compared to peers

Josiah B. Lewis^{a,b}, Melanie E. Fields^{a,b}, Michael M. Binkley^a, Anita Zhou^{a,1}, Amy Mirro^{a,c}, Amy Ouyang^{a,b}, Niket Gupta^{c,2}, Yasheng Chen^a, Slim Fellah^a, Alyssa E. Smith^{a,b}, Igor Dedkov^{a,b}, Monica L. Hulbert^b, Andria L. Ford^{a,c}, Hongyu An^{a,c}, Jin-Moo Lee^{a,c}, Manu S. Goyal^c, Kristin P. Guilliams^{a,b,c,*}

^aDepartment of Neurology, Washington University School of Medicine, 660 S. Euclid Ave., St. Louis, MO, 63110, USA

^bDepartment of Pediatrics, Washington University School of Medicine, 660 S. Euclid Ave., St. Louis, MO, 63110, USA

^cMallinckrodt Institute of Radiology, Washington University School of Medicine, 660 S. Euclid Ave., St. Louis, MO, 63110, USA

Abstract

Children with sickle cell disease (SCD) may develop large vessel narrowing, but studies suggest vessels may also be enlarged, possibly related to increased cerebral blood flow (CBF). We used MRI to investigate whether the cross-sectional total inflow vessel luminal area (TIVLA) proximal to the circle of Willis (carotid arteries + basilar artery) would be increased in SCD compared to age- and sex-matched peers after adjusting for CBF. Across 36 children with SCD (19 female, median age 10.7 [8.0–14.5] years) and 43 controls (26 female, median age 12.7 [9.2–18.2] years) matched by age ($p = 0.13$) and sex ($p = 0.50$), the median TIVLA in the SCD group (35.9 mm² [30.7, 39.5]) was larger than controls (30.5 mm² [27.8, 35.4], $p = 0.002$). In a mixed model including age, sex, hemoglobin, CBF, SCD status, and an interaction between hemoglobin and SCD status, CBF ($\beta = 0.11$, CI 0.02–0.20, $p = 0.02$), SCD ($\beta = 28.02$, CI 5.62–50.42, $p = 0.015$), and the interaction between SCD and hemoglobin ($\beta = -2.48$, CI -4.49 to -0.47, $p = 0.018$)

This is an open access article under the CC BY-NC license (<http://creativecommons.org/licenses/by-nc/4.0/>).

*Corresponding author. Neurology, Pediatrics, and Radiology, Washington University School of Medicine, St. Louis, MO, 63110, USA. kristinguilliams@wustl.edu (K.P. Guilliams).

¹Current address: Department of Pediatrics, University of Nebraska Medical Center, S. 42nd & Emile St., Omaha, NE 68198, USA.

²Current address: Feinberg School of Medicine, Northwestern University, 420 E. Superior St., Chicago, IL 60611, USA.

CRediT authorship contribution statement

Josiah B. Lewis: Writing – review & editing, Writing – original draft, Visualization, Validation, Software, Methodology, Investigation, Formal analysis. **Melanie E. Fields:** Writing – review & editing, Writing – original draft, Investigation. **Michael M. Binkley:** Writing – review & editing, Formal analysis. **Anita Zhou:** Writing – review & editing, Validation, Investigation, Formal analysis. **Amy Mirro:** Writing – review & editing, Software, Investigation. **Amy Ouyang:** Writing – review & editing, Investigation. **Niket Gupta:** Writing – review & editing, Methodology, Investigation. **Yasheng Chen:** Writing – review & editing, Software, Methodology. **Slim Fellah:** Writing – review & editing, Software, Investigation. **Alyssa E. Smith:** Writing – review & editing, Investigation. **Igor Dedkov:** Writing – review & editing, Visualization, Investigation. **Monica L. Hulbert:** Writing – review & editing, Investigation. **Andria L. Ford:** Writing – review & editing, Investigation. **Hongyu An:** Writing – review & editing, Investigation. **Jin-Moo Lee:** Writing – review & editing, Conceptualization. **Manu S. Goyal:** Writing – review & editing, Writing – original draft, Methodology, Investigation, Conceptualization. **Kristin P. Guilliams:** Writing – review & editing, Writing – original draft, Supervision, Project administration, Methodology, Investigation, Conceptualization.

were all significantly associated with increased TIVLA. Notably, TIVLA as a measure of arterial lumens is larger in children with SCD, even after adjusting for CBF in the mixed model. This implies disease-specific normative values may be needed to detect early vasculopathy.

Keywords

Cerebral blood flow; Brain development; Hematology; Cerebrovascular disease; MR angiography; MRI; Arterial spin labeling

1. Introduction

Children with sickle cell disease (SCD), characterized by chronic anemia, are at increased risk for cerebral vasculopathy and neurologic injury. Vasculopathy in SCD is typically characterized by vascular endothelium hyperplasia causing steno-occlusion of the large arteries. Although differing definitions across studies have precluded a unified vasculopathy diagnosis in sickle cell disease, all current definitions use some element of large artery luminal narrowing, typically within the anterior circulation (Guilliams et al., 2019). This steno-occlusive vasculopathy further increases risk for stroke and stroke recurrence in SCD (Guilliams et al., 2017; Hulbert et al., 2011).

One barrier to defining vasculopathy in SCD is a lack of understanding of typical large vessel characteristics and changes in SCD. Recent studies have noted increased vessel lumens in sickle cell disease, possibly as a means to decrease endothelial stress in the presence of higher blood velocity due to anemia (Croal et al., 2017; Václav et al., 2018). Mouse models of SCD have also found degradation of elastin and collagen in the carotid arteries, leading to expansive remodeling of the large vessels (Song et al., 2020). Together, these studies suggest that decreased lumen size may be a late finding in SCD vasculopathy, limiting options for halting further progression of vasculopathy and increasing risk for stroke and brain injury.

As few studies have examined large vessel luminal measurements in the absence of clinically apparent vascular narrowing in children with SCD, we sought to quantify large artery lumen measurements between children with and without SCD in the absence of large vessel vasculopathy. To contextualize lumen measurements within the known alterations of cerebral hemodynamics of SCD, we also sought to examine the relationship of vessel luminal area to CBF. We hypothesized that vessel luminal areas would be increased in children with SCD compared to controls, and larger area would be associated with increased CBF.

2. Materials and methods

2.1. Study design and cohort

The Washington University in St. Louis Institutional Review Board reviewed and approved this study. Informed consent was provided by participants or by legal guardian if the participant was less than 18 years of age upon enrollment. This study used prospectively collected data from research visits of children and young adults with SCD between the ages

of 4 and 30 years old, and healthy siblings and friends without SCD within the same age range, recruited between 2014 and 2021.

Individuals were excluded from participation if they had any form of anemia other than SCD, other neurological or significant systemic illness, had a contraindication or significant artifact (e.g., metal implant or braces, respectively) to magnetic resonance imaging (MRI), were unable to tolerate brain MRI without sedation, had a past medical history including overt stroke, bone marrow transplant, gene therapy, or a clinical diagnosis of cerebral vasculopathy, defined for study purposes as any previously abnormal magnetic resonance angiography (MRA) in the medical record.

2.2. Brain MRI sequences and processing

MRI sequences were collected for each participant without sedation using 3T Siemens Trio or Prisma scanners. Time-of-flight MRA with three-dimensional (3D) readout were collected with a low flip angle of 18° to minimize the effects of intraluminal saturation and were centered on the circle of Willis. Voxel resolution was $\sim 0.6 \times 0.6 \times 0.7 \text{ mm}^3$, or $0.6 \times 0.6 \times 0.6 \text{ mm}^3$ (TE = 3.34, 3.59, or 3.94 ms, TR = 1900–2200 ms). MRAs were visually screened for motion artifacts or field-of-view issues that could affect vessel measurements.

Additional brain MRI sequences included: 3D magnetization prepared rapid gradient echo (MPRAGE) T1-weighted images ($1 \times 1 \times 1 \text{ mm}^3$ voxel resolution, TE/TR = 2.94, 2.95, or 2.97 ms/1800, 1810, or 1820 ms, flip angle = 8° , TI = 1000 ms), processed to segment and measure cortical and white matter volume using the FreeSurfer 5.3 reconstruction pipeline (<https://surfer.nmr.mgh.harvard.edu/fswiki/FreeSurferMethodsCitation>). Fluid attenuated inversion recovery (FLAIR) images (TE/TR = 93 or 94/9000 ms; TI = 2500 ms; flip angle = 150° ; in-plane resolution = $0.86 \times 0.86 \text{ mm}$; slice thickness = 5 mm) were used to assess white matter lesions, manually outlined by a pediatric (K.P.G.) or adult (A.L.F.) vascular neurologist. Pseudo-continuous arterial spin labeling (pCASL) measured CBF with multiple-slice 2-dimensional echo planar imaging (TE/TR = 12 or 13 ms/3280–3840 ms; in-plane voxel resolution = $3 \times 3 \text{ mm}$; slice thickness = 5 mm; 18 slices; 80 measurements; label duration = 1.5 s; post-labeling delay (PLD) = 1.0 or 1.5 s) (Alsop et al., 2015). A single-compartment model was used for CBF quantification. An inversion recovery sequence measured blood T1 within the superior sagittal sinus, allowing for individual CBF quantification, as T1 varies with age and hematocrit (Jain et al., 2012). Whole brain CBF was calculated from voxel-wise, partial volume corrected CBF maps, as previously reported (Fields et al., 2018; Ford et al., 2018; Guillems et al., 2017, 2018). Maps were calculated from 2D-readout pCASL sequences.

In 54 scans, there were two pCASL acquisitions per scan visit, one with a PLD of 1 s, and one with 1.5 s. Comparing these two CBF measurements using a Bland-Altman test (Supplemental Fig. 1(a)) shows linear proportional bias and fixed bias. We determine a simple linear regression model $\text{CBF}_{1.5\text{sPLD}} = 0.762 \times \text{CBF}_{1\text{sPLD}} + 9.126$, $R^2 = 0.929$, predictive error = $\pm 6.2\%$ (CI -10.6 – 13.7%) (Supplemental Fig. 1), similar to previously described methods (Hulbert et al., 2023). Predictive error is calculated using leave-one-out cross-validation (Molinaro et al., 2005). In 28 of the 103 scanning sessions (21 with SCD

and 7 controls) that had 1 s PLD pCASL but not 1.5 s PLD, we used this model to impute the missing 1.5 s PLD, partial volume corrected, whole brain CBF data ($CBF_{1.5sPLD}$).

2.3. Vessel diameter measurements and vessel area calculations

Since blood is delivered to the supratentorial brain through either the anterior (internal carotid arteries) or posterior (basilar artery) circulation, we focused on these inflow vessels. To remain agnostic to the relative contribution of anterior vs. posterior bulk circulation or potential asymmetry within the anterior circulation that may be normalized and redistributed once blood enters the circle of Willis, we measured and summed cross-sectional areas of the internal carotid terminal C7 segments and the distal basilar arteries immediately proximal to the circle of Willis to reflect the total inflow vessel luminal area (TIVLA). Measurements of vessel lumen diameters were made by one of two trained readers (J.L. and A.Z.) using the software RadiAnt DICOM Viewer (Version, 2020.2.3) with the double oblique method and multiplanar reconstruction, as previously described in detail (Guilliams et al., 2021). Briefly, all measurements were collected using the same brightness and contrast to remove inter-rater bias in window selection. Due to issues of partial volume effects at the edges of the vessels, raters drew measurements to capture 2/3rds of the mid-intensity border surrounding the high-intensity vessel cross-section. TIVLA was then calculated as the summed area of the three inflow vessels, where $area = \pi \times (major\ axis\ diameter/2) \times (minor\ axis\ diameter/2)$ (Supplemental Fig. 2).

2.4. Statistical analyses

Baseline continuous variables are presented as median and interquartile range (IQR). Categorical baseline variables are presented as count data and percentage when applicable. Differences in baseline demographics between controls and SCD subjects were compared with the Mann-Whitney *U* test and Chi-squared test for continuous and categorical variables, respectively.

Differences in median TIVLA and CBF between groups were assessed with the Mann-Whitney *U* test. Univariate association between continuous variables of interest (age, TIVLA, hemoglobin, lesion volume, and CBF) was assessed with the Pearson correlation coefficient. A univariate, two-sided significance of less than 0.3 was required for entry into generalized linear mixed models controlling for repeated subject observation. β and 95 % confidence interval (CI) are reported for each variable. Sex and SCD status were retained in the models to adjust for cohort differences in subject population regardless of their significance. Model fit was assessed using the variance inflation factor (VIF) to test for collinearity and the normality of model residuals were evaluated using the Shapiro-Wilk test. A *p*-value of <0.05 was considered significant.

3. Results

3.1. Participants

We acquired MRI scans from 89 participants ages 4–28 years; 6 were excluded because of one or more vessels being outside the field of view of the MRA; and 4 were excluded due to CBF scans failing quality control assessment due to motion. The cohort with complete

data available included 36 participants with SCD, median 10.7 (IQR 8.0, 14.5) years old at baseline timepoint and 43 control participants, median 12.7 (IQR 9.2–18.2) years old ($p = 0.13$). 19 (53 %) of the SCD participants were female, not significantly different than the control participants with 26 (60 %) female ($p = 0.50$). Four participants had three MRI timepoints with available data, 16 participants had two MRI scans in the dataset, and all others had a single scan, for a total of 79 included participants with 103 scans with MRA and CBF acquired. Table 1 records baseline characteristics of the final cohort.

All SCD participants had hemoglobin-SS or S-Beta thal⁰. Twenty-five of the 36 SCD participants were taking hydroxyurea therapy at the baseline scan. Two children who were not taking hydroxyurea at their first scan were on hydroxyurea therapy at their repeat scan, two were on chronic transfusion therapy for frequent/chronic pain, two were on chronic transfusion therapy for abnormal transcranial Doppler ultra-sound (TCD), and one was on chronic transfusion therapy for progression of silent infarcts. All children on chronic transfusion therapy had MRAs for clinical purposes that were read as normal. As shown in Table 1, CBF was higher in children with sickle cell disease than controls ($p < 0.001$).

3.2. Factors influencing total inflow vessel luminal areas

In order to account for the full area of vasculature contributing to intracranial blood flow, the carotid and basilar arteries were summed to calculate TIVLA for each scan. Fig. 1 illustrates basilar artery measurements between representative members of SCD and control cohorts. Group individual artery measurements are shown in Table 1. The median TIVLA was 35.9 mm² in children with SCD (IQR 30.7–39.5), which was significantly larger than the median 30.5 mm² in controls (IQR 27.8–35.4; $p = 0.0018$, Fig. 2).

As time-of-flight signal is flow dependent, with higher flow having better signal-to-noise and brighter intensity, we assessed whether measurement differences in TIVLA could be attributed to flow-dependent artifacts by examining the relationship between our CBF and TIVLA measurements in several ways. First, we compared the ratios of TIVLA/CBF and TIVLA/CBF² between SCD and controls using Mann-Whitney *U*. Both TIVLA/CBF ($p = 0.003$) and TIVLA/CBF² ($p < 0.001$) were significantly different between the cohorts, suggesting that flow artifact was unlikely to be the sole factor causing the difference in measurements. Furthermore, as the proportional relationship between TIVLA and CBF was not consistent across the entire cohort, we treated TIVLA and CBF as related but independent variables in the subsequent analyses.

Second, we compared univariate analyses of TIVLA with age, hemoglobin, white matter lesion volume, and CBF (Fig. 3). Across the entire cohort, TIVLA significantly correlated with CBF ($\rho = 0.48$, $p < 0.001$, Fig. 3(b)) and hemoglobin ($\rho = -0.36$, $p = 0.001$, Fig. 3(c)). Within only the SCD cohort, there was not a correlation between TIVLA and lesion volume ($\rho = -0.02$, $p = 0.92$). Lesions were rarely seen in the control cohort, observed in 4 out of 43 control participants, one of whom contributed 2 scans. Across the entire cohort, 5 control scans contained lesions.

Finally, in a linear mixed model including age, sex, hemoglobin, CBF, SCD status, and an interaction between hemoglobin and SCD status, and adjusting for repeated scans, CBF

($\beta = 0.11$, CI 0.02–0.20, $p = 0.02$, SCD ($\beta = 28.02$, CI 5.62–50.42, $p = 0.02$) and the interaction between SCD and hemoglobin ($\beta = -2.48$, CI -4.49 to -0.47, $p = 0.02$) were all independently associated with TIVLA.

3.3. Factors influencing cerebral blood flow

To further examine the relationship between CBF and vessel size, we examined factors associated with CBF. CBF had significant univariate correlations with TIVLA, age, and hemoglobin (Fig. 3). In a mixed model relating CBF to age, sex, hemoglobin, and TIVLA, age ($\beta = -1.07$, CI -1.60 to -0.54, $p < 0.001$), hemoglobin ($\beta = -3.23$, CI -4.47 to -1.99, $p = 0.001$) and TIVLA ($\beta = 0.64$, CI 0.20–1.08, $p = 0.006$) all remained significant predictors of CBF.

4. Discussion

4.1. Impact of findings

In this study of 79 children with and without sickle cell disease, we found that the total inflow vessel luminal area (TIVLA) is larger in children with SCD without cranial artery stenosis compared to age- and sex-matched controls, even after controlling for differences in CBF. This study adds to a growing body of literature suggesting that vessel narrowing is not the only vascular change in large vessels that impacts children with SCD. Furthermore, when examining the potential role of the vessel lumen in CBF, TIVLA remained a significant predictor of CBF even after adjusting for age and hemoglobin, suggesting that compensatory remodeling may have an adaptive impact on cerebral oxygen delivery beyond those factors currently established influence whole brain perfusion.

4.2. Vascular changes in sickle cell disease

Although lumen-narrowing arteriopathies are the most commonly considered vascular changes in pediatric sickle cell disease, our observation that the vascular lumens in those with SCD are larger than in peers without SCD is consistent with prior studies (Václav et al., 2018). Václav et al. (2018) found increased lumen areas and increased MR-measured blood flow velocity in children and young adults with SCD, both of which were associated with lower hemoglobin. This study noted that the increased luminal area allowed for similar levels of endothelial sheer stress observed in both SCD and control cohorts. Croal et al. (2017) also reported larger MCA vessel diameters in children with SCD than controls, but with the small sample size of 20 total participants, this difference did not reach significance. Our study supports these findings of increased luminal areas in people with SCD; with TIVLA being an independent predictor of cerebral blood flow in our study, suggests that potential SCD-related cerebravascular ectasia warrants further study. In a mouse model of SCD, vessel lumen enlargement was associated with elastin and collagen degradation. Notably, the elastin and collagen degradation was mitigated by inhibiting JNK (c-jun N-terminal kinase) signaling, which led to smaller vessel lumens in the JNK-inhibited SCD mice (Song et al., 2020). If similar mechanisms are found in humans, this may represent a potential therapeutic target to mitigate risk of cerebrovascular injury in people living with SCD.

Interestingly, in non-SCD atherosclerotic disease in adults, where steno-occlusive cerebrovascular disease also increases stroke risk, vessel luminal dilation in the large arteries is one of the earliest markers of vascular dysfunction, preceding vascular lumen narrowing (Labropoulos et al., 1998). Yuan et al. (2021) found children and young adults with SCD had thicker ICA and basilar artery walls with vessel wall imaging. They observed non-significant trends of thicker walls with increasing white blood cell count and decreasing hematocrit, speculating that circulating markers of anemia may be leading to inflammation and remodeling of the vessel walls (Yuan et al., 2021); however, it is unclear if thickening of the vessel walls due to these factors would increase or decrease the inner diameter measured by TOF MRA. Adult studies of carotid diameters in people without SCD but at risk for white matter lesions have found a relationship between increased large vessel diameter and white matter lesion burden. Both the Northern Manhattan Study (Rundek et al., 2017) and a large population study in China (Zhai et al., 2020) found that increased common carotid diameters were associated with increased white matter hyperintensity volume. In our study, children with SCD, who are at risk for silent strokes in the white matter, had larger internal carotid diameters compared to those without SCD. Larger sample sizes and neck vasculature exams are needed to investigate whether a similar relationship between large vessel diameter and white matter lesion burden exists among those with SCD, as we did not find a significant relationship between white matter lesions and TIVLA in our study.

4.3. Changes in cerebral blood flow

Consistent with multiple previous studies in people with and without SCD, we found that age and hemoglobin are significant predictors of cerebral blood flow (Borzage et al., 2016; Goyal et al., 2014; Hurler-Jensen et al., 1994; Prohovnik et al., 1989). We add the contribution of the vascular lumen to CBF, even after controlling for age and hemoglobin. The relationship between age and CBF is related to changes in cerebral metabolism. The brain undergoes dramatic growth and maturation in childhood, with brain volumes peaking early in the 2nd decade of life between ages 11–14 years (Lenroot et al., 2007). In parallel, cerebral oxygen and glucose metabolism rises in childhood, the latter up to 1.5 to 2-fold of typical adult values (Goyal et al., 2014). Even beyond childhood, both age and vascular anatomy contribute to CBF variability in healthy adults (Amin-Hanjani et al., 2015). Cerebral oxygen delivery is the product of cerebral blood flow and arterial oxygen content (total hemoglobin \times percent oxygen saturation of hemoglobin \times constant). It is unsurprising and well established that decreases in hemoglobin lead to increases in cerebral blood flow as the body compensates to maintain a steady oxygen delivery to the brain. However, this vasodilatory compensation is largely presumed to occur on the smaller arteriolar level (Bizeau et al., 2018; Epp et al., 2020), and the potential impact on the large vessels has not been well-described. While the large vessels may need to enlarge to compensate for the increased bulk flow and endothelial shear stress (Guilliams et al., 2021), if the increased vessel area was only a passive accommodation for cerebral oxygen delivery, we would expect that the ratio of TIVLA/CBF would be similar between the groups, or that vessel area would lose significance after adjusting for hemoglobin, neither of which is true in our data. The persistence of TIVLA in the CBF model after adjustment for hemoglobin suggests that hemoglobin and inflow area represent unique components affected in the SCD population, warranting further investigation.

The relationship between flow and area is dependent on velocity, and cerebral blood flow velocity is a known important risk factor for overt stroke development in sickle cell disease (Adams et al., 1998, 1992; Adams et al., 1992). We did not directly measure blood flow velocity at the time of CBF and MRA in this study, and there is not a clear correlation between TCD velocities and cerebral blood flow, unless both patient-specific vessel areas and estimated weight of tissue perfused by the insonated vessel are captured to allow conversion of the TCD measurement into similar units of cerebral blood flow (Croal et al., 2017). This underscores the importance of vessel area in understanding cerebrovascular hemodynamics in SCD. There is currently wide variation in whether duplex, a.k.a. imaging, or non-duplex TCD is used for sickle cell disease screening (Schlenz et al., 2020). Non-duplex and duplex have different thresholds recommended for initiating stroke prevention interventions (DeBaun et al., 2020). Future work could consider whether imaging TCD-measured vessels may find similarly increased vessel area in SCD and whether this adds value to current TCD screening thresholds.

In summary, this cross-sectional study cannot fully explain why TIVLA is increased in SCD beyond the portion of the increase due to a heightened CBF. This unexplained proportion of increased TIVLA may be an appropriately adaptive to decrease the resistance of higher cerebral blood flow. Indeed, one of the hallmarks of the vasculature is the ability to adapt and dilate or constrict to regulate pressure, shear stress, resistance, and flow.

There are many interrelated abnormalities of vascular function in SCD that may influence changes in TIVLA. Increased WBC adhesion to endothelium, intravascular hemolysis, and dysregulated coagulation activation are all potential contributors to vascular dysfunction in SCD (Kato et al., 2009). The viscosity of Hb S-containing blood is higher than non-Hb S blood at an equivalent hematocrit, which may contribute to alterations in cerebral blood flow and endothelial damage (Connes et al., 2016). Over time, these chronic abnormalities could lead to pathological vascular remodeling including loss of collagen and elastin. It is known that children (Fox et al., 2022) and adults with SCD (Nabavizadeh et al., 2016) are at high risk for cerebral aneurysms, which could be a late consequence of chronic vascular dilatation and vessel wall thinning.

4.4. Limitations

This study has several limitations. First, larger cohorts, particularly with longitudinal data, will likely elucidate the relationship between vasculature changes and CBF in SCD. Second, while time-of-flight MRA is commonly used clinically to look for vascular abnormalities including in children with SCD, this technique is limited in spatial resolution and potential artifacts related to high blood flow velocities. “Black-blood” sequences such as SPACE that suppress the blood flow signal (Mandell et al., 2017) can help to overcome these limitations and are needed to confirm the current findings. However, our main findings of increased diameter are consistent with other studies reporting increased diameter in SCD, and we would not expect vessel diameter to retain significance for predicting SCD while controlling for CBF if it were merely an indirect marker of increased CBF. Third, we do not have a single PLD across the entire cohort. However, when we examined the data just in the 52 children (72 scans) with 1s PLD CBF data, all models retained similar significant variables

with only minor differences in exact estimates (Supplemental Fig. 3). Finally, we do not have simultaneous TCD or other measurements of velocity to fully explain the relationship between vessel area and blood flow. We presume that all children had normal TCD velocities at the time of scanning, as children with SCD were recruited from clinic where this is monitored regularly. Moreover, this information would not change the conclusions that vessel area is likely associated with CBF variability. Future studies combining CBF measurements, dedicated vessel wall imaging, and velocities across childhood would help further clarify these relationships.

4.5. Conclusion

Children with SCD have larger TIVLA compared to age- and sex-matched controls. Larger TIVLA is independently associated with higher global CBF, even after adjusting for age and hemoglobin. Together these findings suggest that SCD causes increased luminal area in cerebral large vessels, and that this increased area is unlikely to be only a biomarker of anemia but may have its own impact on cerebral hemodynamics independent of hemoglobin. Further research is needed to understand the mechanism of increased vessel area and the potential need for disease-specific normative values for early detection of vasculopathy.

Supplementary Material

Refer to Web version on PubMed Central for supplementary material.

Acknowledgements

The authors would like to acknowledge research coordinators Luisa Gil Diaz, Madison Streb, Rachel Shields, and Liam Comiskey for their role in participant recruitment and coordination of study visits, and the staff at the Center for Clinical Imaging Research for assistance with scan acquisition.

This work is supported by the National Institutes of Health (NIH), Eunice Kennedy Shriver National Institute of Child Health and Human Development (K12 HD04734) (K.P.G.) Intellectual and Developmental Disabilities Research Center at Washington University (U54 HD087011) (K.P.G.); Washington University St. Louis CTSA from the NIH, National Center for Advancing Translational Sciences (UL1 TR000448) (K.P.G. and M.E.F.); Hematology K12 (5K12HL2087107) (M.E.F.); NIH, National Institute of Neurological Disorders and Stroke grants K23NS099472 (K.P.G.), R01NS121065 (K.P.G.) R01NS085419 (J.M.L.), and R01NS082561 (H.A.); NIH, National Heart, Lung, and Blood Institute grant R01HL129241 (A.L.F.), R01HL157188 (M.E.F.).

Declaration of competing interest

MLH: Pfizer: Spouse employment and scientific advisory board participation. Novartis: Research funding to the institution. Bluebird Bio: Consulting.

Data availability

The data that support the findings of this study are available from the corresponding author upon reasonable request.

References

Adams RJ, McKie VC, Hsu L, Files B, Vichinsky E, Pegelow C, Abboud M, Gallagher D, Kutlar A, Nichols FT, Bonds DR, Brambilla D, 1998. Prevention of a first stroke by transfusions in children with sickle cell anemia and abnormal results on transcranial Doppler ultrasonography. *N. Engl. J. Med* 339, 5–11. 10.1056/NEJM199807023390102. [PubMed: 9647873]

- Adams RJ, Nichols FT, Figueroa R, McKie V, Lott T, 1992. Transcranial Doppler correlation with cerebral angiography in sickle cell disease. *Stroke* 23, 1073–1077. 10.1161/01.str.23.8.1073. [PubMed: 1636180]
- Adams Robert, Virgil McKie, Fenwick Nichols, Elizabeth Carl, Dao-Long Zhang, Kathy McKie, Figueroa Ramon, Mark Litaker, Thompson William, Hess David, 1992. The use of transcranial ultrasonography to predict stroke in sickle cell disease. *N. Engl. J. Med* 326, 605–610. 10.1056/NEJM199202273260905. [PubMed: 1734251]
- Alsop DC, Detre JA, Golay X, Günther M, Hendrikse J, Hernandez-Garcia L, Lu H, MacIntosh BJ, Parkes LM, Smits M, van Osch Matthias J.P., Wang Danny J.J., Wong EC, Zaharchuk G, 2015. Recommended implementation of arterial spin-labeled perfusion MRI for clinical applications: a consensus of the ISMRM perfusion study group and the European consortium for ASL in dementia. *Magn. Reson. Med* 73, 102–116. 10.1002/mrm.25197. [PubMed: 24715426]
- Amin-Hanjani S, Du X, Pandey DK, Thulborn KR, Charbel FT, 2015. Effect of age and vascular anatomy on blood flow in major cerebral vessels. *J. Cerebr. Blood Flow Metab. Off. J. Int. Soc. Cerebr. Blood Flow Metab* 35, 312–318. 10.1038/jcbfm.2014.203.
- Bizeau A, Gilbert G, Bernier M, Huynh MT, Bocti C, Descoteaux M, Whittingstall K, 2018. Stimulus-evoked changes in cerebral vessel diameter: a study in healthy humans. *J. Cerebr. Blood Flow Metabol* 38, 528–539. 10.1177/0271678X17701948.
- Borzage MT, Bush AM, Choi S, Nederveen AJ, Václav L, Coates TD, Wood JC, 2016. Predictors of cerebral blood flow in patients with and without anemia. *J. Appl. Physiol. Bethesda Md* 120, 976–981. 10.1152/jappphysiol.00994.2015.
- Connes P, Alexy T, Deterich J, Romana M, Hardy-Dessources M-D, Ballas SK, 2016. The role of blood rheology in sickle cell disease. *Blood Rev.* 30, 111–118. 10.1016/j.blre.2015.08.005. [PubMed: 26341565]
- Croal PL, Leung J, Kosinski P, Shroff M, Odame I, Kassner A, 2017. Assessment of cerebral blood flow with magnetic resonance imaging in children with sickle cell disease: a quantitative comparison with transcranial Doppler ultrasonography. *Brain Behav* 7, e00811. 10.1002/brb3.811. [PubMed: 29201539]
- DeBaun MR, Jordan LC, King AA, Schatz J, Vichinsky E, Fox CK, McKinstry RC, Telfer P, Kraut MA, Daraz L, Kirkham FJ, Murad MH, 2020. American Society of Hematology 2020 guidelines for sickle cell disease: prevention, diagnosis, and treatment of cerebrovascular disease in children and adults. *Blood Adv.* 4, 1554–1588. 10.1182/bloodadvances.2019001142. [PubMed: 32298430]
- Epp R, Schmid F, Weber B, Jenny P, 2020. Predicting vessel diameter changes to up-regulate biphasic blood flow during activation in realistic microvascular networks. *Front. Physiol* 11. 10.3389/fphys.2020.566303.
- Fields ME, Williams KP, Ragan DK, Binkley MM, Eldeniz C, Chen Y, Hulbert ML, McKinstry RC, Shimony JS, Vo KD, Doctor A, An H, Ford AL, Lee J-M, 2018. Regional oxygen extraction predicts border zone vulnerability to stroke in sickle cell disease. *Neurology* 90, e1134–e1142. 10.1212/WNL.0000000000005194. [PubMed: 29500287]
- Ford AL, Ragan DK, Fella S, Binkley MM, Fields ME, Williams KP, An H, Jordan LC, McKinstry RC, Lee J-M, DeBaun MR, 2018. Silent infarcts in sickle cell disease occur in the border zone region and are associated with low cerebral blood flow. *Blood* 132, 1714–1723. 10.1182/blood-2018-04-841247. [PubMed: 30061156]
- Fox CK, Leykina L, Hills NK, Kwiatkowski JL, Kanter J, Strouse JJ, Voeks JH, Fullerton HJ, Adams RJ, Post-STOP Study Group, 2022. Hemorrhagic stroke in children and adults with sickle cell anemia: the post-STOP cohort. *Stroke* 53, e463–e466. 10.1161/STROKEAHA.122.038651. [PubMed: 36205141]
- Goyal MS, Hawrylycz M, Miller JA, Snyder AZ, Raichle ME, 2014. Aerobic glycolysis in the human brain is associated with development and neotenus gene expression. *Cell Metab.* 19, 49–57. 10.1016/j.cmet.2013.11.020. [PubMed: 24411938]
- Williams KP, Fields ME, Dowling MM, 2019. Advances in understanding ischemic stroke physiology and the impact of vasculopathy in children with sickle cell disease. *Stroke* 50, 266–273. 10.1161/STROKEAHA.118.020482. [PubMed: 30661504]
- Williams KP, Fields ME, Ragan DK, Chen Y, Eldeniz C, Hulbert ML, Binkley MM, Rhodes JN, Shimony JS, McKinstry RC, Vo KD, An H, Lee J-M, Ford AL, 2017. Large-vessel vasculopathy

in children with sickle cell disease: a magnetic resonance imaging study of infarct topography and focal atrophy. *Pediatr. Neurol* 69, 49–57. 10.1016/j.pediatrneurol.2016.11.005. [PubMed: 28159432]

- Guilliams KP, Fields ME, Ragan DK, Eldeniz C, Binkley MM, Chen Y, Comiskey LS, Doctor A, Hulbert ML, Shimony JS, Vo KD, McKinstry RC, An H, Lee J-M, Ford AL, 2018. Red cell exchange transfusions lower cerebral blood flow and oxygen extraction fraction in pediatric sickle cell anemia. *Blood* 131, 1012–1021. 10.1182/blood-2017-06-789842. [PubMed: 29255068]
- Guilliams KP, Gupta N, Srinivasan S, Binkley MM, Ying C, Couture L, Gross J, Wallace A, McKinstry RC, Vo K, Lee J-M, An H, Goyal MS, 2021. MR imaging differences in the Circle of Willis between healthy children and adults. *AJNR Am. J. Neuroradiol* 42, 2062–2069. 10.3174/ajnr.A7290. [PubMed: 34556478]
- Hulbert ML, Fields ME, Guilliams KP, Bijlani P, Shenoy S, Fellah S, Towerman AS, Binkley MM, McKinstry RC, Shimony JS, Chen Y, Eldeniz C, Ragan DK, Vo K, An H, Lee J-M, Ford AL, 2023. Normalization of cerebral hemodynamics after hematopoietic stem cell transplant in children with sickle cell disease. *Blood* 141, 335–344. 10.1182/blood.2022016618. [PubMed: 36040484]
- Hulbert ML, McKinstry RC, Lacey JL, Moran CJ, Panepinto JA, Thompson AA, Sarnaik SA, Woods GM, Casella JF, Inusa B, Howard J, Kirkham FJ, Anie KA, Mullin JE, Ichord R, Noetzel M, Yan Y, Rodeghier M, Debaun MR, 2011. Silent cerebral infarcts occur despite regular blood transfusion therapy after first strokes in children with sickle cell disease. *Blood* 117, 772–779. 10.1182/blood-2010-01-261123. [PubMed: 20940417]
- Hurler-Jensen AM, Prohovnik I, Pavlakis SG, Piomelli S, 1994. Effects of total hemoglobin and hemoglobin S concentration on cerebral blood flow during transfusion therapy to prevent stroke in sickle cell disease. *Stroke* 25, 1688–1692. 10.1161/01.str.25.8.1688. [PubMed: 8042222]
- Jain V, Duda J, Avants B, Giannetta M, Xie SX, Roberts T, Detre JA, Hurt H, Wehrli FW, Wang DJJ, 2012. Longitudinal reproducibility and accuracy of pseudo-continuous arterial spin-labeled perfusion MR imaging in typically developing children. *Radiology* 263, 527–536. 10.1148/radiol.12111509. [PubMed: 22517961]
- Kato GJ, Hebbel RP, Steinberg MH, Gladwin MT, 2009. Vasculopathy in sickle cell disease: biology, pathophysiology, genetics, translational medicine and new research directions. *Am. J. Hematol* 84, 618–625. 10.1002/ajh.21475. [PubMed: 19610078]
- Labropoulos N, Zarge J, Mansour MA, Kang SS, Baker WH, 1998. Compensatory arterial enlargement is a common pathobiologic response in early atherosclerosis. *Am. J. Surg* 176, 140–143. 10.1016/S0002-9610(98)00135-4. [PubMed: 9737619]
- Lenroot RK, Gogtay N, Greenstein DK, Wells EM, Wallace GL, Clasen LS, Blumenthal JD, Lerch J, Zijdenbos AP, Evans AC, Thompson PM, Giedd JN, 2007. Sexual dimorphism of brain developmental trajectories during childhood and adolescence. *Neuroimage* 36, 1065–1073. 10.1016/j.neuroimage.2007.03.053. [PubMed: 17513132]
- Mandell DM, Mossa-Basha M, Qiao Y, Hess CP, Hui F, Matouk C, Johnson MH, Daemen M.J.a.P., Vossough A, Edjlali M, Saloner D, Ansari SA, Wasserman BA, Mikulis DJ, Vessel Wall Imaging Study Group of the American Society of Neuroradiology, 2017. Intracranial vessel wall MRI: principles and expert consensus recommendations of the American Society of Neuroradiology. *AJNR Am. J. Neuroradiol* 38, 218–229. 10.3174/ajnr.A4893. [PubMed: 27469212]
- Molinaro AM, Simon R, Pfeiffer RM, 2005. Prediction error estimation: a comparison of resampling methods. *Bioinformatics* 21, 3301–3307. 10.1093/bioinformatics/bti499. [PubMed: 15905277]
- Nabavizadeh SA, Vossough A, Ichord RN, Kwiatkowski J, Pukenas BA, Smith MJ, Storm PB, Zager EL, Hurst RW, 2016. Intracranial aneurysms in sickle cell anemia: clinical and imaging findings. *J. Neurointerventional Surg* 8, 434–440. 10.1136/neurintsurg-2014-011572.
- Prohovnik I, Pavlakis SG, Piomelli S, Bello J, Mohr JP, Hilal S, De Vivo DC, 1989. Cerebral hyperemia, stroke, and transfusion in sickle cell disease. *Neurology* 39, 344–348. 10.1212/wnl.39.3.344. [PubMed: 2927641]
- Rundek T, Della-Morte D, Gardener H, Dong C, Markert MS, Gutierrez J, Roberts E, Elkind MSV, DeCarli C, Sacco RL, Wright CB, 2017. Relationship between carotid arterial properties and cerebral white matter hyperintensities. *Neurology* 88, 2036–2042. 10.1212/WNL.0000000000003951. [PubMed: 28446647]

- Schlenz AM, Phillips S, Mueller M, Melvin C, Adams RJ, Kanter J, Investigators, DISPLACE, 2020. Practice patterns for stroke prevention using transcranial Doppler in sickle cell anemia: DISPLACE Consortium. *Pediatr. Blood Cancer* 67, e28172. 10.1002/pbc.28172. [PubMed: 31925913]
- Song H, Keegan PM, Anbazhakan S, Rivera CP, Feng Y, Omojola VO, Clark AA, Cai S, Selma J, Gleason RL, Botchwey EA, Huo Y, Tan W, Platt MO, 2020. Sickle cell anemia mediates carotid artery expansive remodeling that can be prevented by inhibition of JNK (c-jun N-terminal kinase). *Arterioscler. Thromb. Vasc. Biol* 40, 1220–1230. 10.1161/ATVBAHA.120.314045. [PubMed: 32160775]
- Václav L, Baldew ZAV, Gevers S, Mutsaerts HJMM, Fijnvandraat K, Cnossen MH, Majoie CB, Wood JC, VanBavel E, Biemond BJ, van Ooij P, Nederveen AJ, 2018. Intracranial 4D flow magnetic resonance imaging reveals altered haemodynamics in sickle cell disease. *Br. J. Haematol* 180, 432–442. 10.1111/bjh.15043. [PubMed: 29270975]
- Yuan S, Jordan LC, Davis LT, Cogswell PM, Lee CA, Patel NJ, Waddle SL, Juttukonda M, Sky Jones R, Griffin A, Donahue MJ, 2021. A cross-sectional, case-control study of intracranial arterial wall thickness and complete blood count measures in sickle cell disease. *Br. J. Haematol* 192, 769–777. 10.1111/bjh.17262. [PubMed: 33326595]
- Zhai F-F, Yang M, Wei Y, Wang M, Gui Y, Han F, Zhou L-X, Ni J, Yao M, Zhang S-Y, Jin Z-Y, Cui L-Y, Dai Q, Zhu Y-C, 2020. Carotid atherosclerosis, dilation, and stiffness relate to cerebral small vessel disease. *Neurology* 94. 10.1212/WNL.0000000000009319 e1811–e1819. [PubMed: 32241954]

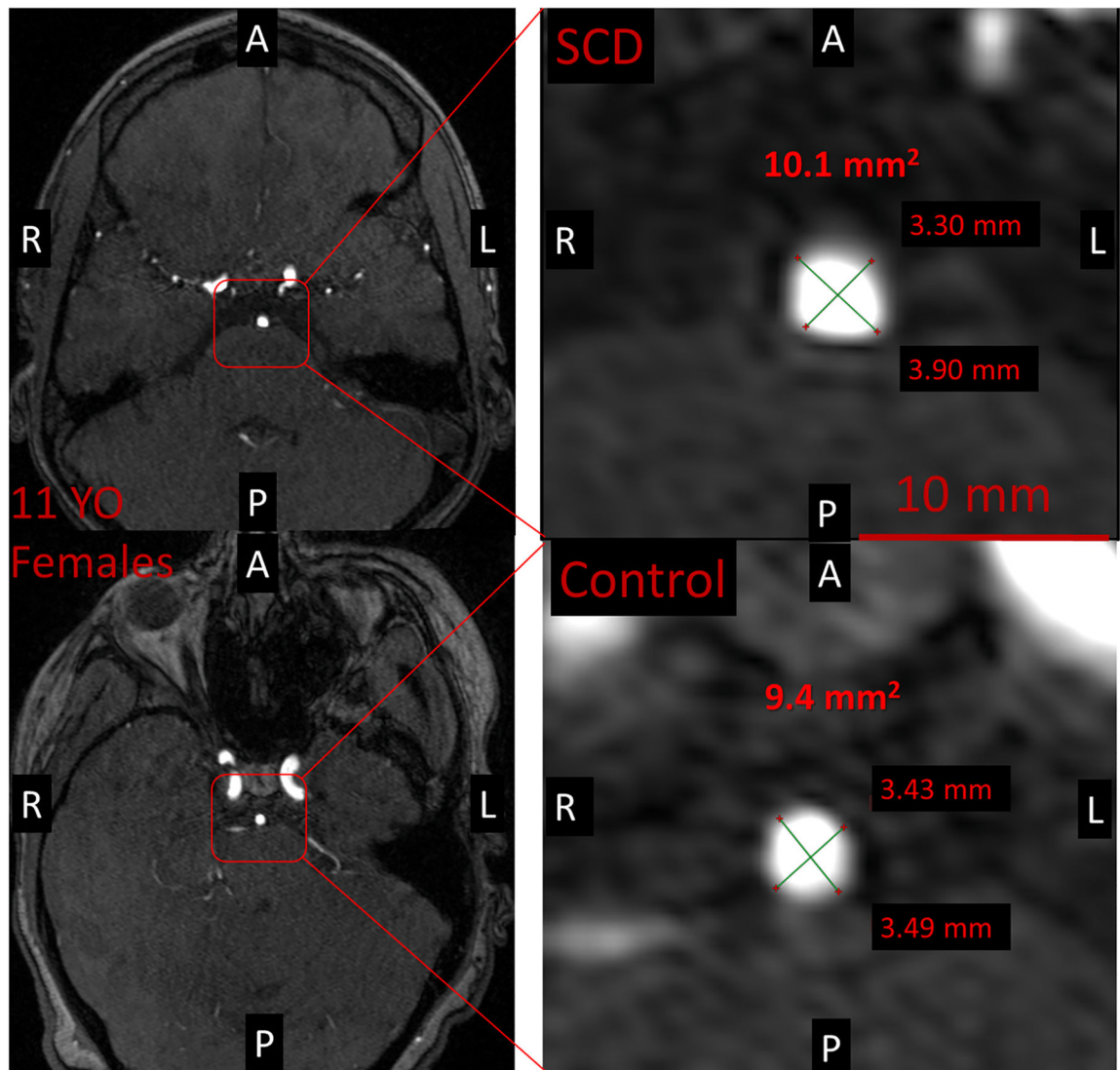


Fig. 1. Comparison of distal basilar cross-sectional area between representative subjects: both 11-year-old females, one with SCD (top), the other a control (bottom). TOF-MRA axial slices (left) and zoomed basilar region (right). The area of the distal basilar segment for the SCD participant is ~7 % higher, and the TIVLA is ~20 % higher.

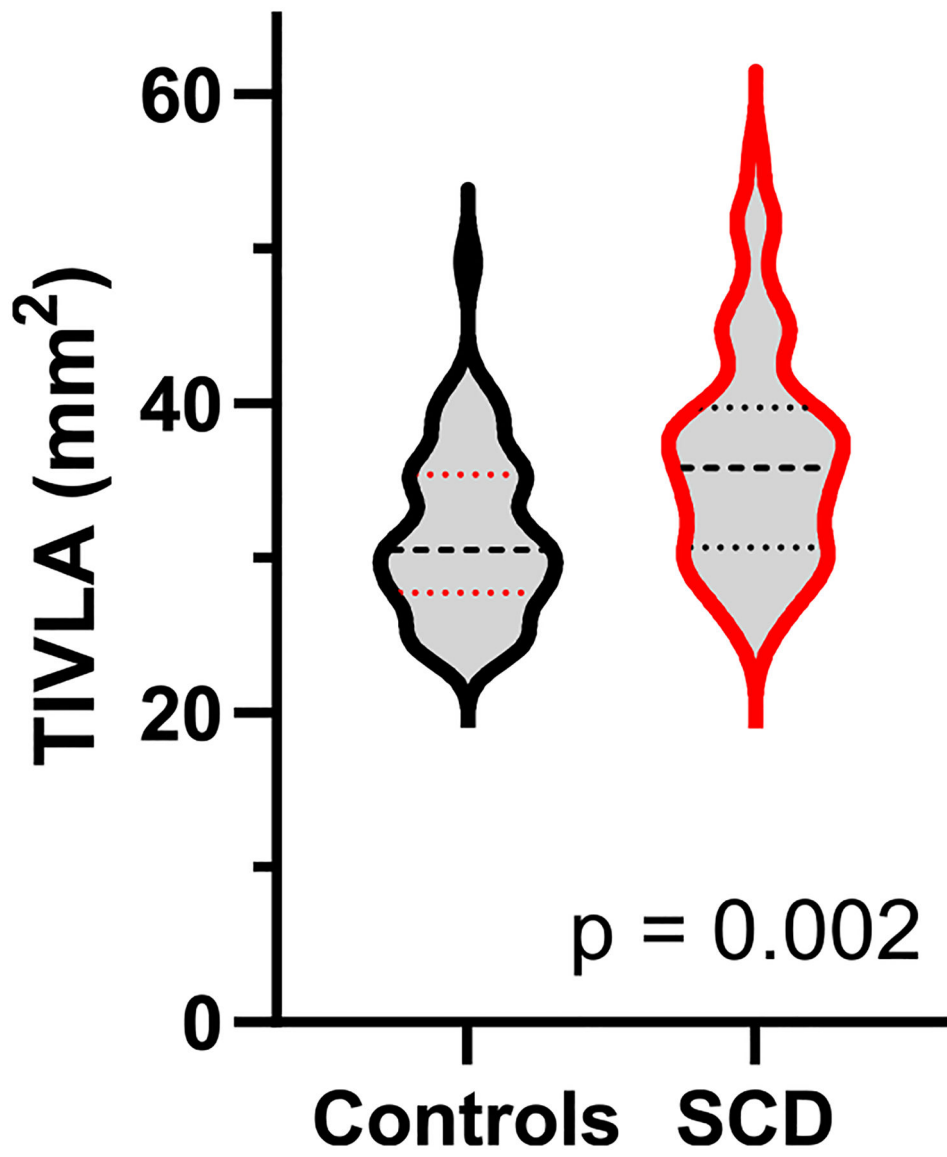


Fig. 2. Density 'violin' plot showing TIVLA from SCD and control cohorts. Median values are represented by coarsely dashed lines, interquartile ranges by finely dashed lines.

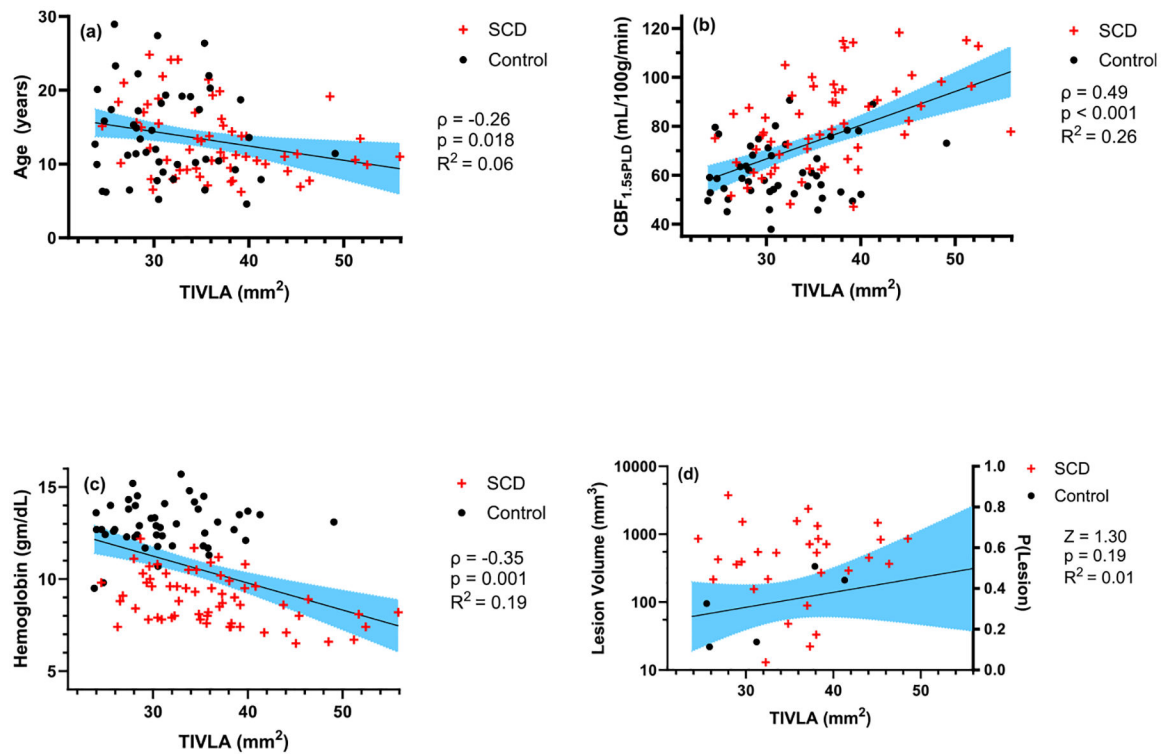


Fig. 3. Univariate correlations with Pearson correlation coefficients (ρ), significance (p), and linear regression (R^2) showing (a) age, (b) whole brain cerebral blood flow, and (c) hemoglobin against TIVLA. Lesion volume is also plotted against TIVLA, along with a fit to the probability of having a lesion volume of any size detected, with Wilcoxon Z (d). 95 % confidence intervals are plotted in blue.

Table 1
Baseline median and interquartile range, except for sex, which is reported as the number and percentage of female participants.

Variable	Whole Cohort (N = 79)	SCD (N = 36)	Controls (N = 43)	p-value ^b
Age (y)	11.4 [8.3, 16.3]	10.7 [8.0, 14.5]	12.7 [9.2, 18.2]	0.13
Sex, Female (%)	45 (57)	19 (53)	26 (60)	0.50
Race	57	36	21	
African-American	16	0	16	
Caucasian	2	0	2	
Asian	3	0	3	
Other	2	0	2	
Ethnicity	77	36	41	
Hispanic				
Non-Hispanic				
Hemoglobin (g/dl)	11.70 [8.90, 12.90]	8.8 [7.9, 9.7]	12.8 [12.29, 13.80]	<0.001
Cerebral Blood Flow (mL/100 g/min)	71.2 [57.9, 82.5]	82.8 [70.7, 95.7]	59.7 [52.9, 72.6]	<0.001
Inflow Area (mm ²)	32.5 [28.5, 38.1]	35.9 [30.7, 39.5]	30.5 [27.8, 35.4]	0.002
Right C7 Dia. ^a (mm)	3.8 [3.4, 4.1]	4.0 [3.5, 4.2]	3.6 [3.4, 4.0]	0.10
Left C7 Dia. ^a (mm)	3.9 [3.6, 4.1]	4.0 [3.6, 4.2]	3.8 [3.5, 4.1]	0.06
Distal Bas. Dia. ^a (mm)	3.7 [3.4, 3.9]	3.8 [3.6, 4.3]	3.5 [3.3, 3.7]	<0.001
Lesion Volume (cc)	0 [0, 22]	6.5 [0, 480]	0 [0.00, 0.00]	<0.001

^aDia. = Diameter: mean of major and minor axes measured in ellipsoidal cross-section.

^bp-values are two-sided and are calculated using the Mann-Whitney *U* test.